

The *Synechocystis* PCC6803 MerA-Like Enzyme Operates in the Reduction of Both Mercury and Uranium under the Control of the Glutaredoxin 1 Enzyme

Benoit Marteyn,^{a*} Samer Sakr,^a Sandrine Farci,^a Mariette Bedhomme,^b Solenne Chardonnet,^c Paulette Decottignies,^c Stéphane D. Lemaire,^b Corinne Cassier-Chauvat,^a Franck Chauvat^a

UMR8221, CEA, CNRS, Université Paris Sud, iBiTec-S, LBBC, Gif sur Yvette, France^a; CNRS, Université Pierre et Marie Curie, Institut de Biologie Physico-Chimique, Laboratoire de Biologie Moléculaire et Cellulaire des Eucaryotes, FRE3354, Paris, France^b; CNRS/Université Paris-Sud, Institut de Biochimie et Biophysique Moléculaire et Cellulaire, UMR8619, Orsay, France^c

In a continuing effort to analyze the selectivity/redundancy of the three glutaredoxin (Grx) enzymes of the model cyanobacterium *Synechocystis* PCC6803, we have characterized an enzyme system that plays a crucial role in protection against two toxic metal pollutants, mercury and uranium. The present data show that Grx1 (Slr1562 in CyanoBase) selectively interacts with the presumptive mercuric reductase protein (Slr1849). This MerA enzyme plays a crucial role in cell defense against both mercuric and uranyl ions, in catalyzing their NADPH-driven reduction. Like MerA, Grx1 operates in cell protection against both mercury and uranium. The Grx1-MerA interaction requires cysteine 86 (C86) of Grx1 and C78 of MerA, which is critical for its reductase activity. MerA can be inhibited by glutathionylation and subsequently reactivated by Grx1, likely through deglutathionylation. The two Grx1 residues C31, which belongs to the redox active site (CX₂C), and C86, which operates in MerA interactions, are both required for reactivation of MerA. These novel findings emphasize the role of glutaredoxins in tolerance to metal stress as well as the evolutionary conservation of the glutathionylation process, so far described mostly for eukaryotes.

Cyanobacteria, the very abundant photosynthetic prokaryotes which support much of the life on Earth in using solar energy to produce oxygen and biomass for the food chain, are continuously challenged with the toxic reactive oxygen species (ROS) generated by their respiration and photosynthesis. Among other processes, these ROS impair the redox homeostasis of cellular thiols, which can be subsequently restored by the thioredoxin and glutaredoxin systems (1). In the glutaredoxin system (2), NADPH is used to sequentially reduce (i) the glutathione reductase (GR) enzyme present in many, but not all (3), organisms; (ii) the glutathione (GSH) tripeptide; and (iii) the glutaredoxin (Grx) enzymes, which can also be reduced by the thioredoxin reductase enzymes (3–5). Grxs are widely conserved proteins that comprise two main families: the dithiol enzymes with a CX₂C redox center (where C stands for cysteine and X stands for any other amino acid) and the monothiol enzymes with a CX₂S redox-active center (where S stands for serine). The dithiol Grxs catalyze the reduction of disulfides (protein-S-S) or glutathione mixed disulfide (protein-S-SG) by a dithiol (CX₂C-requiring) or a monothiol (CX₂S-dependent) mechanism. In contrast, monothiol Grxs operate in the sensing of cellular iron and in the biogenesis of iron-sulfur clusters that play crucial roles in electron transfer processes (6–8). Some monothiol Grxs have also been reported to catalyze protein deglutathionylation (5, 9). However, the selectivity/redundancy of the Grx enzymes is poorly understood for photosynthetic organisms, even for cyanobacteria that possess a small number of Grxs (1), compared to plants (10). Whereas *Arabidopsis thaliana* has 31 Grxs (10), the model cyanobacterium *Synechocystis* PCC6803 (here *Synechocystis*) has only one monothiol Grx (11) and two dithiol enzymes (1). These two dithiol Grxs, Grx1 and Grx2, were shown to specifically interact with various proteins operating in tolerance to arsenate (12) and selenate (3).

In this study, we pursued the analysis of the Grx enzymes,

emphasizing their possible role in protection against mercury (13) and uranium (14), which are massively used by human industries, leading to pollutions (15–17). Grx1 (Slr1562 in CyanoBase [<http://genome.kazusa.or.jp/cyanobase/>]), but neither Grx2 nor Grx3, appeared to interact with the Slr1849 protein, which is presented as a presumptive mercuric reductase (MerA) enzyme in CyanoBase. This MerA-like protein was found to operate in the protection against, and the NADPH-driven reduction of, not only mercuric but also uranyl ions (thereby challenging the notion of metal selectivity). Hence, cyanobacterial enzymes like MerA with the capacity to remediate both mercury and uranium might be interesting for future utilization of cyanobacteria for bioremediation (18), as most polluted sites contain cocktails of toxic metals. Consistent with the MerA-Grx1 interaction, Grx1 appeared to be crucial for protection against both mercury and uranium, like MerA. Furthermore, the activity of MerA was found to be inhibited by glutathionylation (formation of a glutathione mixed disulfide between a Cys residue of the protein and the Cys residue of glutathione) and subsequently reactivated by Grx1, likely through a deglutathionylation process. These findings emphasize the evolutionary conservation of the glutathionylation/deglutathionylation

Received 11 March 2013 Accepted 7 July 2013

Published ahead of print 12 July 2013

Address correspondence to Franck Chauvat, franck.chauvat@cea.fr.

* Present address: Benoit Marteyn, Unité de Pathogénie Microbienne Moléculaire, Institut Pasteur, Paris, France.

B.M. and S.S. contributed equally to this work.

Supplemental material for this article may be found at <http://dx.doi.org/10.1128/JB.00272-13>.

Copyright © 2013, American Society for Microbiology. All Rights Reserved.
doi:10.1128/JB.00272-13

control of enzyme activity, a biological process described mostly for eukaryotes (19, 20).

MATERIALS AND METHODS

Microbial strains, growth conditions, and gene transfer procedures. *Synechocystis* PCC6803 (here *Synechocystis*) was grown at 30°C or 39°C (depending on the strain) on mineral medium (MM) derived from BG11 (21), as described previously (22). For plate assays, 10- μ l aliquots of 10-fold serial dilutions of mid-log-phase cultures (2.5×10^7 cells \cdot ml $^{-1}$) were spotted onto solid MM with or without the indicated concentration of HgCl $_2$ and UO $_2$ (CH $_3$ COO) $_2$, which were incubated for 5 to 7 days prior to image acquisition. *Escherichia coli* strains used for gene manipulations (HB101, XL1-Blue MRF', and TOP10 [Invitrogen]), production of recombinant proteins [BL21(DE3) (Novagen) and KY2266 (23)], two-hybrid assays (DHM1 [24]), or conjugation (CM404) of *Synechocystis* (22) were grown on LB medium at 30°C (CM404 and KY2266) or 37°C (all other strains). Antibiotics used for selection were as follows: ampicillin (Ap) at 100 μ g \cdot ml $^{-1}$, chloramphenicol (Cm) at 50 μ g \cdot ml $^{-1}$, kanamycin (Km) at 50 μ g \cdot ml $^{-1}$, nalidixic acid at 20 μ g \cdot ml $^{-1}$, and spectinomycin (Sp) at 100 μ g \cdot ml $^{-1}$ for *E. coli*, and Cm at 10 μ g \cdot ml $^{-1}$, Km at 50 to 300 μ g \cdot ml $^{-1}$, Sp at 5 μ g \cdot ml $^{-1}$, and streptomycin (Sm) at 5 μ g \cdot ml $^{-1}$ for *Synechocystis*.

Gene cloning and manipulation. *Synechocystis* DNA was PCR amplified with specific primers to generate the studied genes without or with their two flanking genomic regions for homologous recombinations mediating targeted gene replacement upon transformation (25). After cloning into the appropriate plasmids (Table 1), the studied protein-coding sequences were either mutagenized (QuikChange mutagenesis kit; Stratagene) or replaced by an antibiotic-resistant marker inserted in the same orientation. These constructions were verified by PCR and DNA sequencing (BigDye kit; ABI Perkin-Elmer), before and after propagation in *Synechocystis*. PCR was also used to assay whether segregation between the wild-type (WT) and mutant copies of the polyploid (25) chromosome was complete (the studied gene is dispensable for cell growth) or not (the gene is essential for cell viability).

Analysis of protein-protein interactions with the bacterial two-hybrid system. Each *Synechocystis* full-length coding sequence was translationally fused to the intrinsically inactive adenylate cyclase (AC) domains of the replication-compatible plasmids pKT25 and pUT18, which were subsequently doubly transformed into *E. coli* reporter strain DHM1 to search for AC reconstitution, which turns on β -galactosidase production (24), generating the blue color of the cells grown during 2 days at 30°C on indicator plates containing 5-bromo-4-chloro-3-indolyl- β -D-galactopyranoside (X-gal) (40 mg \cdot ml $^{-1}$; Eurobio), isopropyl-1-thio- β -D-galactopyranoside (IPTG) (0.5 mM; Invitrogen), Ap, Km, and nalidixic acid. β -Galactosidase (β -Gal) activity was measured as described previously (3). One β -Gal unit is equal to 1 nmol *o*-nitrophenyl- β -D-galactopyranoside (ONPG) min $^{-1}$ \cdot mg $^{-1}$ protein.

Overproduction of affinity-tagged proteins and GST pull-down. The coding sequence of each studied protein was PCR amplified and tagged by cloning into the appropriate *E. coli* vectors (Table 1). The resulting plasmids were introduced into *E. coli* strain BL21(DE3) for the production of recombinant proteins tagged with either 6 \times His or glutathione *S*-transferase (GST) or into triple-protease-defective mutant strain KY2266 (23) for the production of the maltose-binding protein (MBP)-tagged MerA protein. Cells grown at 30°C for 2 h (up to an optical density at 600 nm [OD $_{600}$] of 0.5 to 0.7) were induced with 0.5 to 1 mM IPTG for 4 to 12 h at 30°C, washed, and resuspended in 2 ml of lysis buffer (10 mM Tris-HCl [pH 7.4], 150 mM NaCl, 10% glycerol, and 1% IGEPAL; Sigma) for the purification of 6 \times His-tagged proteins. In contrast, 2 ml of PBS (10 mM phosphate buffer [pH 7.4], 120 mM NaCl, 2.7 mM KCl, 1 mM phenylmethylsulfonyl fluoride [PMSF], 10 mM dithiothreitol [DTT], and 0.1% Triton X-100) was used for the purification of GST-tagged proteins, and 5 ml buffer A (30 mM Tris-HCl [pH 8], 200 mM NaCl) was used for MBP-MerA purification.

Cells were then rapidly frozen in an Eaton press chamber cooled in a dry ice ethanol bath, disrupted (250 MPa), and centrifuged at 14,000 \times g for 30 min at 4°C (22) to collect the supernatant (about 1.5 ml) containing the soluble proteins. For the purification of the MBP-MerA fusion protein, the supernatant was loaded onto a 1-ml amylose resin column (New England BioLabs) preequilibrated and washed (10 bed volumes) with buffer A. Following elution with 10 mM maltose (Sigma) in buffer A, the purity of MBP-MerA, checked by SDS-PAGE, was >90%. The MBP tag was then cleaved (factor Xa protease; New England BioLabs) and removed by anion-exchange chromatography (Bio-Rad). The presence of MerA in the eluted fractions was confirmed by mass spectrometry analysis on a matrix-assisted laser desorption ionization-time of flight (MALDI-TOF) apparatus after trypsin cleavage (peptide mass fingerprint), and its concentration was determined spectrophotometrically by using its calculated molar extinction coefficient at 280 nm (30,470 M $^{-1}$ \cdot cm $^{-1}$). Purified MerA was concentrated in 30 mM Tris-HCl (pH 8)–200 mM NaCl with Amicon Ultra centrifugation filters (Millipore) and briefly stored at –80°C prior to analysis.

6 \times His-tagged proteins were purified on Ni-nitrilotriacetic acid (NTA) agarose beads (Qiagen) and eluted with lysis buffer containing 200 mM imidazole. For GST pull-down analysis, 1 μ g of GST-tagged Grx1 was immobilized on glutathione-Sepharose beads (Pharmacia) and incubated with 80 μ l of cell extract (10 mg of proteins) containing MerA-6 \times His in 900 μ l of binding buffer (20 mM HEPES [pH 6.8], 100 mM KCl, 5 mM MgCl $_2$, 2% glycerol, 1 mM DTT, 1 mM PMSF, and 1 mM EDTA) for 2 h at 4°C under continuous rotation. Beads collected by centrifugation were washed three times (Qiagen buffer), resuspended in 50 μ l of binding buffer, and boiled for 5 min in sample buffer prior to SDS-PAGE (16% polyacrylamide). The purity of the studied proteins was >90%.

Mercuric and uranyl reductase activities. Mercuric reductase activity was assayed (26) at 37°C with a solution containing 80 mM sodium phosphate (pH 7.4), 200 μ M NADPH, 1 mM 2-mercaptoethanol, 2 μ M flavin adenine dinucleotide (FAD), and 100 μ M HgCl $_2$ on either *Synechocystis* cell extracts or 0.5 μ M purified MerA. The activity was monitored for 2 min as the decrease in A $_{340}$ (molar extinction coefficient of 6,200 M $^{-1}$ \cdot cm $^{-1}$) attributable to NADPH oxidation. As indicated, HgCl $_2$ was replaced by UO $_2$ (CH $_3$ COO) $_2$ (200 μ M), and MerA was either reduced by a 15-min treatment at 22°C with 10 mM DTT in Tris-HCl (pH 8) or glutathionylated by a 30-min incubation with 20 mM oxidized glutathione (GSSG) followed by filtration and resuspension in phosphate buffer prior to the enzyme assay (27). When required, 0.5 μ M Grx1 (WT or mutants) or Grx2 and 1 mM reduced glutathione (GSH) were added to the reaction mixture. One unit of reductase activity is defined as the amount of enzyme that catalyzes the oxidation of 1.0 μ mol NADPH per min.

Production of biotinylated glutathione. The water-soluble biotinylation reagent EZ Link Sulfo-NHS-Biotin (Perbio Science) was used to couple biotin to the primary amino group of GSSG, as described previously (28). The biotinylation reagent (40 μ l; 48 mM) was incubated with GSSG (40 μ l; 32 mM) in 50 mM potassium phosphate buffer (pH 7.2) for 1 h at room temperature, generating biotinylated GSSG (BioGSSG). Free biotin was then quenched by adding 28 μ l of 0.6 M ammonium carbonate (NH $_4$ HCO $_3$).

In vitro glutathionylation of MerA with BioGSSG. MerA was reduced with 50 mM DTT, desalted in 30 mM Tris-HCl (pH 8)–200 mM NaCl with NAP-5 columns (GE Healthcare), treated or not with 100 mM iodoacetamide (IAM) and 20 mM *N*-ethylmaleimide (NEM) as alkylating agents for 30 min in the dark, and then incubated for 1 h with 2 mM BioGSSG in 30 mM Tris-HCl (pH 7.9). As indicated, the reversibility of the glutathionylation treatment was checked with a 30-min incubation with 50 mM DTT. All treatments were performed at room temperature. Proteins were then loaded onto nonreducing SDS-PAGE gels and analyzed by Western blotting using anti-biotin antibodies, as described previously (28).

TABLE 1 Characteristics of the plasmids used in this study

Plasmid	Relevant feature(s) ^a	Reference or source
Analysis of protein-protein interactions with the bacterial two-hybrid system		
pUT18	Amp ^r plasmid encoding the T18 domain of the <i>Bordetella pertussis</i> adenylate cyclase in frame with an upstream multiple-cloning site	24
pKT25	Km ^r plasmid encoding the T25 domain of the <i>B. pertussis</i> adenylate cyclase in frame with a downstream multiple-cloning site	24
pUT18- <i>zip</i>	pUT18 with the CS for the self-interacting Zip control protein	24
pKT25- <i>zip</i>	pKT25 with the CS for the self-interacting Zip control protein	24
pUT18- <i>merA</i>	pUT18 with the full-length <i>Synechocystis merA</i> CS (slr1849)	This study
pKT25- <i>merA</i>	pKT25 with the full-length <i>Synechocystis merA</i> CS	This study
pUT18- <i>arsC</i>	pUT18 with the full-length <i>Synechocystis arsC</i> CS (slr0946)	This study
pKT25- <i>arsC</i>	pKT25 with the full-length <i>Synechocystis arsC</i> CS	This study
pUT18- <i>grx1</i>	pUT18 with the full-length <i>Synechocystis grx1</i> CS (slr1562)	3
pKT25- <i>grx1</i>	pKT25 with the full-length <i>Synechocystis grx1</i> CS	3
pUT18- <i>grx2</i>	pUT18 with the full-length <i>Synechocystis grx2</i> CS (ssr2061)	3
pKT25- <i>grx2</i>	pKT25 with the full-length <i>Synechocystis grx2</i> CS	3
pUT18- <i>grx3</i>	pUT18 with the full-length <i>Synechocystis grx3</i> CS (slr1846)	This study
pKT25- <i>grx3</i>	pKT25 with the full-length <i>Synechocystis grx3</i> CS	This study
Gene inactivation in <i>Synechocystis</i>		
pGEMT	Amp ^r AT overhang cloning vector	Promega
pUC4K	Source of the Km ^r marker gene	Pharmacia
pHP45Ω	Source of the Sm ^r Sp ^r marker gene	39
pΔgrx1::Km ^r	Km ^r cassette for deletion of the <i>grx1</i> CS	3
pΔgrx2::Sm ^r /Sp ^r	Sm ^r Sp ^r for deletion of the <i>grx2</i> CS	3
pmerA	pGEMT with the 534-bp <i>merA</i> CS preceded by its 177-bp upstream region	This study
pΔmerA::Km ^r	pmerA with the Km ^r marker in a SmaI site created at 84 bp of MerA CS	This study
Gene expression in <i>Synechocystis</i>		
pFC1	Replicating plasmid for heat-inducible gene expression in <i>Synechocystis</i>	32
pFmerA	pFC1 with the <i>merA</i> CS cloned between NdeI and EcoRI for heat-inducible production of MerA	This study
pSB2A	Replicating plasmid for expressing genes from their own promoter	34
pSmerA	pSB2A expressing the <i>merA</i> gene from its 150-bp promoter region	This study
pSmerA _{C78S}	pSmerA where cysteine 78 of MerA is replaced by a serine	This study
pSgrx1	pSB2A expressing the <i>grx1</i> gene from its 150-bp promoter region	This study
pSgrx1 _{C86S}	pSgrx1 where cysteine 86 of Grx1 is replaced by a serine	This study
Protein production in <i>E. coli</i>		
pET21b(+)	Plasmid for fusion of the 6×His tag at the C terminus of proteins	Novagen
pETM30	Plasmid for fusion of the GST tag at the N terminus of proteins	Novagen
pTrc2	Plasmid for fusion of the cMyc and 6×His tags at the C terminus of proteins	Invitrogen
pgrx1-6His	pET21b(+) with the <i>grx1</i> CS cloned at the NdeI-EcoRI sites	This study
pgrx1-6His _{C31S}	pgrx1-6His with the C31S mutation in <i>grx1</i>	This study
pgrx1-6His _{C86S}	pgrx1-6His with the C86S mutation in <i>grx1</i>	This study
pmerA-6His	pTrc2 with the <i>merA</i> CS cloned at the BamHI-EcoRI sites	This study
pmerA _{C78S} -6His	pmerA-6His harboring the C78S mutation in <i>merA</i>	This study
pgrx2-6His	pTrc2 with the <i>grx2</i> CS cloned at the BamHI-EcoRI sites	This study
pGST-grx1	pETM30 with the <i>grx1</i> CS cloned at the SalI-XhoI sites	This study
pMaL-c2	Plasmid for fusion of the MBP tag at the C terminus of proteins	New England BioLabs
pSS9	pMaL-c2 with the <i>merA</i> CS cloned at the EcoRI-BamHI sites	This study

^a CS, coding sequence.

RESULTS

Characterization of a specific interaction between Grx1 and the presumptive mercuric reductase (MerA) with a bacterial two-hybrid system and identification of crucial amino acid residues in each partner. To search for new protein targets of the three Grxs of *Synechocystis* PCC6803 (*Synechocystis*), we used the bacterial adenylate cyclase two-hybrid (BACTH) system (24), which works well in our hands (3, 29). Therefore, the full-length coding

sequences of the dithiol glutaredoxins (3) Grx1 (Slr1562 in CyanoBase) and Grx2 (Ssr2061) and the monothiol enzyme (11) Grx3 (Slr1846) were cloned into the two BACTH reporter plasmids pUT18 and pKT25 (Table 1). The resulting plasmids, pUT18-Grx and pKT25-Grx, were independently used as baits to identify pairwise interactions restoring the production of the β-galactosidase reporter enzyme. Two percent of the thousand protein-protein interaction tests that were performed turned out

TABLE 2 Identification and analysis of protein-protein interactions with the BACTH system^a

Coding sequence cloned into pUT18	Coding sequence cloned into pKT25	Mean β -Gal activity (U) \pm SD
Controls		
Zip	Zip	4,236 \pm 113
None	None	94 \pm 11
<i>grx1</i>	None	67 \pm 18
None	<i>grx1</i>	68 \pm 15
<i>grx2</i>	None	72 \pm 11
None	<i>grx2</i>	77 \pm 08
<i>grx3</i>	None	93 \pm 10
None	<i>grx3</i>	67 \pm 08
None	<i>arsC</i>	89 \pm 17
<i>merA</i>	None	74 \pm 13
Tests		
<i>grx1</i>	<i>arsC</i>	97 \pm 14
<i>grx2</i>	<i>arsC</i>	1,687 \pm 138
<i>merA</i>	<i>grx1</i>	1,836 \pm 97
<i>merA</i>	<i>grx2</i>	65 \pm 12
<i>merA</i>	<i>grx3</i>	74 \pm 12
<i>merA</i>	<i>grx1</i> _{Q29L}	1,071 \pm 47
<i>merA</i>	<i>grx1</i> _{C31S} *	2,161 \pm 25
<i>merA</i>	<i>grx1</i> _{C34S} *	1,221 \pm 54
<i>merA</i>	<i>grx1</i> _{K52A}	39 \pm 05
<i>merA</i>	<i>grx1</i> _{TV72SL}	1,838 \pm 87
<i>merA</i>	<i>grx1</i> _{C86S}	292 \pm 14
<i>merA</i>	<i>grx1</i> _{Q97L}	308 \pm 13
<i>merA</i> _{E70A}	<i>grx1</i>	64 \pm 12
<i>merA</i> _{C78S} *	<i>grx1</i>	93 \pm 16
<i>merA</i> _{C83S} *	<i>grx1</i>	2,096 \pm 182
<i>merA</i> _{C205S}	<i>grx1</i>	1,411 \pm 62
<i>merA</i> _{D246A}	<i>grx1</i>	1,974 \pm 179
<i>merA</i> _{C345S}	<i>grx1</i>	1,689 \pm 134

^a The occurrence of interactions between the proteins produced from the pUT18 and pKT25 reporter plasmids cotransformed into *E. coli* was ascertained by measuring the β -galactosidase activity (1 β -Gal unit corresponds to hydrolysis of 1 nmol *o*-nitrophenyl- β -D-galactopyranoside \cdot min⁻¹ \cdot mg⁻¹ of protein). The numbers are the mean values \pm standard deviations from six assays (three measurements performed on two different cell extracts). The Zip-containing and empty plasmids served as positive and negative controls, respectively (24). The nature and position of amino acid substitutions are indicated by the subscripts. The presumed redox-active cysteines are indicated by asterisks.

to be positive (data not shown). As a positive-control test, we verified (Table 2) that the BACTH system was able to detect the interaction between Grx2 and ArsC (Slr0946), the arsenate reductase enzyme (12). This finding gave us confidence in the novel interaction reported here (Table 2) between Grx1 and the presumptive mercuric reductase protein MerA (Slr1849), a well-conserved protein in cyanobacteria (see Fig. S1 in the supplemental material). The MerA-Grx1 interaction appeared to be specific, as MerA interacted with neither Grx2 nor Grx3 (Table 2).

To strengthen confidence in the Grx1-MerA interaction, interaction-disruptive amino acid substitutions we searched for, focusing on cysteine (C) residues because they can be critical for the activity of Grxs (30) and bacterial MerA enzymes (31). Hence, the cysteine residues of Grx1 and MerA were independently replaced by a serine (S). In addition, several charged amino acids were independently replaced by neutral ones. The results led to the identification of amino acids critical for the Grx1-MerA interac-

tion (Table 2) in both the Grx1 (C86, K52, and Q97) and MerA (C78 and E70) protein partners.

Validation of the Grx1-MerA interaction with GST pull-down assays and confirmation of the crucial role of amino acids C86 of Grx1 and C78 of MerA. The Grx1-MerA interaction detected with the two-hybrid test (Table 2) was confirmed with a GST pull-down assay. First, the GST and 6 \times His tags allowing facile protein purification were fused to the N terminus of Grx1 (GST-Grx1) and the C terminus of MerA (MerA-6 \times His), respectively. The pull-down assay then showed the MerA-6 \times His protein to be retained by the GST-Grx1 hybrid protein but not by the GST protein alone (Fig. 1). Furthermore, the same mutations, C86S in Grx1 and C78S in MerA (Fig. 1), abolished the Grx1-MerA interaction detected with both the two-hybrid test (Table 2) and the GST pull-down (Fig. 1).

The MerA protein operates in the protection of *Synechocystis* against both mercury and uranium. To investigate the role of the MerA-like protein in the fitness of *Synechocystis*, a *merA* deletion cassette (Δ *merA*::Km^r) (Table 1) was constructed and introduced by transformation into *Synechocystis*. The transformant clones retained no wild-type (WT) copies of the chromosome, which is polyploid (25), showing that MerA is dispensable for cell growth under standard laboratory conditions. The *merA* null mutant appeared to be more sensitive to mercuric ions (Hg²⁺) than the WT strain (Fig. 2), showing that MerA operates in protection against mercury. Having noticed the high level of sequence homology (55% identities and 71% similarities) between the MerA-like proteins from *Synechocystis* and the uranium-tolerant bacterium *Geobacter uraniireducens* (GenBank accession number ZP_01142587), we tested whether the *Synechocystis* MerA-like protein might operate in protection against uranyl ions (UO₂²⁺) as well. Indeed, the *merA* null mutant (Δ *merA*::Km^r) was less tolerant to UO₂²⁺ than the WT strain (Fig. 2). These data were confirmed as follows. First, the *merA* protein-coding sequence (Table 1) was cloned into plasmid pFC1, which replicates autonomously in various hosts, including *Synechocystis* (32, 33). pFC1 harbors the λ cl₈₅₇ gene, encoding the temperature-sensitive repressor that tightly controls the activity of the otherwise strong λ p_R promoter located downstream, which is followed by the λ cro ribosome-binding site (5'-AGGA-3') and an ATG start codon (in boldface type) embedded within the unique NdeI restriction site (5'-CATATG-3') for in-frame fusion of the studied protein-coding sequences. Hence, using pFC1, the production of the studied proteins is strongly dependent on the growth temperature (high-level production at 39°C, moderate-level of production at 34°C, and absence of production at 30°C). The results showed that a moderate heat induction of MerA production in cells incubated at 34°C increased their resistance to both mercury and uranium

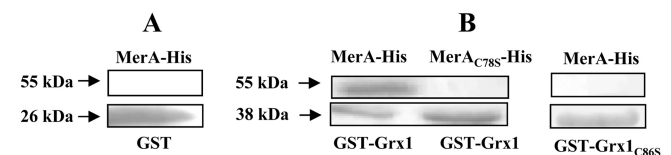


FIG 1 GST pull-down analysis of the MerA-Grx1 interaction. The GST (26 kDa) (A), GST-Grx1 (38 kDa) (B), or GST-Grx1_{C86S} (38 kDa) (B) protein, independently linked to GSH-Sepharose beads, was incubated with *Synechocystis* cell extracts containing either the MerA-His (55 kDa) or MerA_{C78S}-His (55 kDa) protein, and the protein complex was analyzed by SDS-PAGE and Coomassie blue staining. Arrows point to the migration of studied proteins. This experiment was performed twice.

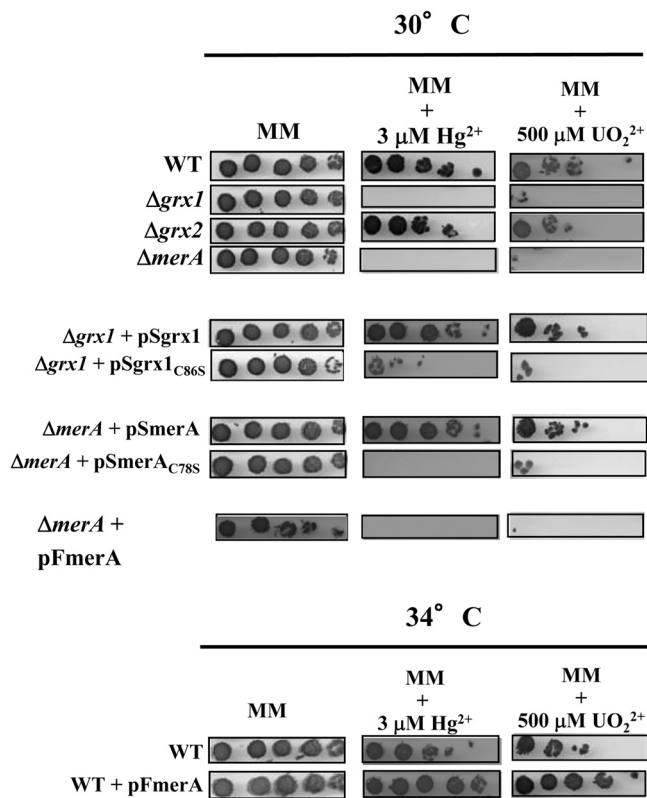


FIG 2 Influence of mercury and uranium on growth of various *Synechocystis* strains. Tenfold serial dilutions of mid-log-phase cultures were spotted onto MM plates with or without Hg^{2+} (HgCl_2) ($3 \mu\text{M}$) or UO_2^{2+} [$\text{UO}_2(\text{CH}_3\text{CO}_2)_2$] ($500 \mu\text{M}$) and subsequently incubated for 4 to 5 days prior to image acquisition. The strains are indicated as WT (wild type), $\Delta merA$ (*merA* null mutant), $\Delta grx1$ (*grx1* null mutant), and $\Delta grx2$ (*grx2* null mutant). The complementation tests of the null mutants were performed at 30°C with the pSB2A replicating plasmid that expressed either the *merA* gene (pSmerA) or its C78S mutant allele (pSmerA_{C78S}), or the *grx1* gene (pSgrx1) or its mutant allele (pSgrx1_{C86S}). The overexpression tests were done at 34°C with WT cells propagating the pFmerA replicating plasmid that expressed the *merA* coding sequence under the control of a temperature-regulated promoter. These experiments were repeated three times.

(Fig. 2). Second, the *merA* gene expressed from its own promoter (Table 1) was cloned into our pSB2A plasmid that replicates at the same 10 copies per cell (34) as the polyploid chromosome (25). The resulting plasmid, pSmerA, was introduced and stably propagated in the *merA* null mutant, yielding $\Delta merA::\text{Km}^r/\text{pSmerA}$ cells, which expressed *merA* at a natural level and displayed the WT level of tolerance to both Hg^{2+} and UO_2^{2+} , as expected (Fig. 2). Collectively, these data demonstrate that MerA operates in protection of *Synechocystis* against both mercury and uranium.

The conserved C78 residue of the MerA protein of *Synechocystis* is crucial to cell protection against mercury and uranium. The same plasmid strategy was used to test the influence of the C78 residue of MerA, which belongs to its presumptive redox-active site ($\text{C}_{78}\text{X}_4\text{C}_{83}$, conserved in cyanobacteria) (see Fig. S1 in the supplemental material), on cell tolerance to mercury and uranium. The *merA*_{C78S} mutant allele was cloned into pSB2A and subsequently introduced into the *merA* null mutant. The resulting $\Delta merA::\text{Km}^r/\text{pSmerA}_{\text{C78S}}$ strain remained as sensitive to both Hg^{2+} and UO_2^{2+} as its parental *merA* null mutant (Fig. 2). This finding shows that the

conserved C78 residue of MerA is crucial to MerA-driven protection of *Synechocystis* against both mercury and uranium.

Enzymological confirmation that the *Synechocystis* MerA enzyme possesses a NADPH-driven mercuric/uranyl reductase activity requiring C78 of its conserved CX_4C redox-active motif. MerA proteins with or without the C78S mutation were produced in *E. coli* as recombinant fusion proteins with a C-terminal 6×His tag for facile purification (Table 1). A classical test that measures the NADPH-driven reduction of mercuric ions (26) was then used to show that the *Synechocystis* MerA protein was able to catalyze the NADPH-dependent reduction of not only mercuric but also uranyl ions (Table 3). MerA activity appeared to be increased by the full reduction of MerA with DTT prior to the enzyme assay (Table 3). In contrast, MerA activity was abolished by the C78S mutation of its conserved redox-active cysteine (Table 3), which decreased MerA-driven cell protection against both Hg^{2+} and UO_2^{2+} (Fig. 2).

Grx1 is involved in the defense of *Synechocystis* against both mercury and uranium, like MerA. The presently reported MerA-Grx1 interaction led us to speculate that Grx1 might also be involved in resistance to both mercury and uranium. The *grx1* null mutant ($\Delta grx1::\text{Km}^r$) (Table 1), which is as fit as the WT strain in the absence of stress (3), was found to be more sensitive to both Hg^{2+} and UO_2^{2+} than WT cells (Fig. 2). To confirm that this phenotype can be rescued by Grx1, the *grx1* gene was cloned into the pSB2A vector, and the resulting pSgrx1 plasmid (Table 1) was introduced in the *grx1* null mutant. The resulting $\Delta grx1::\text{Km}^r/\text{pSgrx1}$ cells displayed WT levels of tolerance to Hg^{2+} and UO_2^{2+} (Fig. 2). Together, these data show that Grx1 operates in cell protection against both mercury and uranium, like MerA. In contrast, Grx2, which does not interact with MerA (Table 2), appeared to be dispensable for tolerance to Hg^{2+} and UO_2^{2+} (Fig. 2).

In vivo evidence that MerA needs to interact with Grx1 in order to protect cells against mercury and uranium. The role of

TABLE 3 *In vitro* assay of MerA-like activity^a

Reaction mixture	Mean NADPH consumption (nmol · min ⁻¹ · mg ⁻¹ of protein) ± SD
MerA + HgCl_2	32.0 ± 0.3
MerA _{C78S} + HgCl_2	1.0 ± 0.1
MerA + $(\text{CH}_3\text{COO})_2\text{UO}_2$	9.7 ± 2.9
MerA _{C78S} + $(\text{CH}_3\text{COO})_2\text{UO}_2$	1.2 ± 0.4
MerA reduced form + HgCl_2	75.0 ± 0.5
MerA glutathionylated form + HgCl_2	2.2 ± 0.1
MerA glutathionylated form + Grx1 reduced form + HgCl_2	48.2 ± 0.6
MerA glutathionylated form + Grx1 _{C86S} reduced form + HgCl_2	4.3 ± 0.1
MerA glutathionylated form + Grx1 _{C31S} reduced form + HgCl_2	1.6 ± 0.1
MerA glutathionylated form + Grx2 reduced form + HgCl_2	3.2 ± 0.1

^a The activity of the *Synechocystis* MerA-like enzyme was measured as the consumption of NADPH (nmol · min⁻¹ · mg⁻¹ of protein) that reduces mercuric or uranyl ions. As indicated, MerA was either reduced or glutathionylated and subsequently treated or not treated with Grx1 or Grx2 before the reactions were started. The nature and position of amino acid substitutions in MerA and Grx1 are shown as subscripts. The numbers are the mean values ± standard deviations from four assays (two measurements performed on two independent enzyme preparations). The negative-control experiments performed in the absence of either NADPH, MerA, or mercuric or uranyl ions yielded only background values (1 to 3 units).

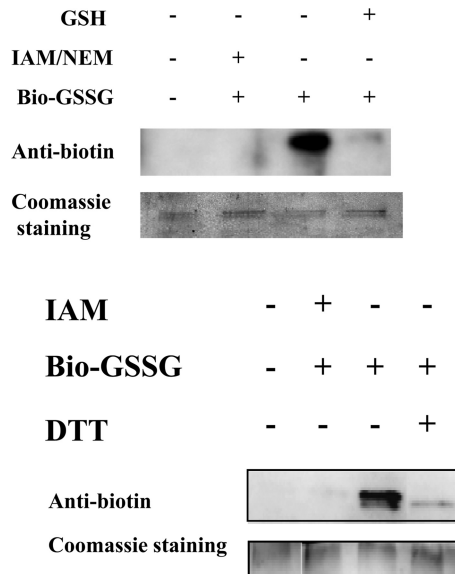


FIG 3 Analysis of MerA glutathionylation with biotinylated glutathione (BioGSSG). Prereduced MerA was incubated for 1 h in the presence of BioGSSG (2 mM) with or without prior incubation with both 2-iodoacetamide (IAM) (100 mM) and *N*-ethylmaleimide (NEM) (20 mM). The reversibility of the glutathionylation of MerA was assessed by treatment with dithiothreitol (DTT) (50 mM). Proteins were resolved by nonreducing SDS-PAGE and transferred onto nitrocellulose for Western blotting with anti-biotin antibodies. Coomassie staining of the gel shows equal loading in each lane. The results of two independent tests are shown.

the MerA-Grx1 interaction in the defense against mercury and uranium was tested as follows. The *grx1*_{C86S} mutant gene encoding the Grx1_{C86S} protein, which was unable to interact with MerA (Table 2 and Fig. 2), was cloned into plasmid pSB2A. The resulting plasmid, pSgrx1_{C86S}, was introduced into the Hg- and U-sensitive *grx1* null mutant, yielding the Δ *grx1*::Km^r/pSgrx1_{C86S} strain. These cells remained sensitive to both Hg²⁺ and UO₂²⁺, unlike the Δ *grx1*::Km^r/pSgrx1 strain. These findings showed that the *grx1*_{C86S} mutant gene had lost the ability of the WT *grx1* allele to restore tolerance to Hg²⁺ and UO₂²⁺ to *grx1* null cells (Fig. 2). Together, these data show that the Grx1 interaction with MerA is required for tolerance to both Hg²⁺ and UO₂²⁺.

MerA activity is impaired by glutathionylation and subsequently restored by Grx1, which likely catalyzes MerA deglutathionylation. The interaction between the Grx2 and ArsC enzymes (Table 2) is consistent with a previous *in vitro* report that ArsC can be glutathionylated upon arsenate reduction and subsequently reactivated through deglutathionylation catalyzed by the *E. coli* GrxA enzyme (35). By analogy with these data, the presently described MerA-Grx1 interaction led us to speculate that MerA might be glutathionylated upon Hg²⁺ reduction and subsequently deglutathionylated by Grx1. Hence, using standard *in vitro* procedures to assay glutathionylation (27, 28), MerA was incubated with biotinylated glutathione (BioGSSG). Subsequently, the presence of glutathione adducts on MerA was analyzed by Western blotting using an anti-biotin antibody (Fig. 3). A clear signal was observed for the BioGSSG-treated MerA protein, which completely disappeared after subsequent reduction with DTT treatment (Fig. 3). Furthermore, MerA glutathionylation (MerASSG) was confirmed by showing that it could be prevented (Fig. 3) by

MerA pretreatment with the specific cysteine-alkylating agents iodoacetamide (IAM) and *N*-ethylmaleimide (NEM), known to impair glutathionylation. Also, interestingly, MerA glutathionylation was shown to inhibit MerA activity, which could be restored subsequently by Grx1 (Table 3). The redox-active C31 residue of Grx1 was crucial for Grx1-mediated reactivation of MerA. Similarly, the C86 residue of Grx1, critical for the MerA-Grx1 interaction (Table 2 and Fig. 1 and 2), was also required for MerA reactivation (Table 3). To confirm the positive influence of Grx1 on MerA activity, we compared the levels observed in cell extracts prepared from the WT strain and the *grx1* null mutant (Δ *grx1*::Km^r). As expected, WT cells displayed higher-level mercuric and uranyl reductase activities than *grx1* null cells (Table 4). Collectively, these data indicate that MerA can be inactivated by glutathionylation and subsequently reactivated by Grx1, which likely catalyzes MerA deglutathionylation. In contrast, Grx2 could not reactivate glutathionylated MerA (Table 3), in agreement with the absence of a Grx2-MerA interaction (Table 2) and the dispensability of Grx2 for cell protection against Hg²⁺ (Fig. 2).

DISCUSSION

We pursued the analysis of the widely conserved glutaredoxins (Grxs) in the model cyanobacterium *Synechocystis* PCC6803, which possesses two dithiol enzymes (Grx1 [Slr1562] and Grx2 [Ssr2061]) (3, 12) and one monothiol Grx (Grx3 [Slr1846]) (11). The bacterial two-hybrid system (24), which worked well in our hands (3, 29), was used to search for proteins selectively interacting with only one Grx. Grx1, but neither Grx2 nor Grx3, was found to interact with the Slr1849 protein (Table 2). This protein, highly conserved in cyanobacteria (see Fig. S1 in the supplemental material), with the exceptions of *Prochlorococcus* and marine *Synechococcus* species, is homologous to the bacterial mercuric reductase enzyme MerA (<http://genome.kazusa.or.jp/cyanobase/>). The Grx1-MerA interaction was confirmed with GST pulldown assays (Fig. 1) and the identification of critical amino acids in each partner, such as the C86 residue of Grx1 and the C78 residue of MerA (Table 2 and Fig. 1). Through gene deletion and plasmid complementation analyses (Fig. 2) with replicative vectors (32, 34), MerA was found to be (i) dispensable for cell growth in the absence of stress and (ii) crucial to cell defense against mercuric ions (HgCl₂).

TABLE 4 Analysis of MerA-like activity of *Synechocystis* cell extracts prepared from the WT strain and the Grx1 null mutant^a

Reaction mixture	Mean NADPH consumption (%) \pm SD
WT + DTT + HgCl ₂	100.0
WT + HgCl ₂	83.7 \pm 8.1
Δ <i>grx1</i> + DTT + HgCl ₂	74.2 \pm 7.3
Δ <i>grx1</i> + HgCl ₂	27.5 \pm 3.3
WT + DTT + (CH ₃ COO) ₂ UO ₂	100.0
WT + (CH ₃ COO) ₂ UO ₂	98.0 \pm 9.1
Δ <i>grx1</i> + DTT + (CH ₃ COO) ₂ UO ₂	78.6 \pm 7.3
Δ <i>grx1</i> + (CH ₃ COO) ₂ UO ₂	27.8 \pm 3.3

^a The activity of the *Synechocystis* MerA-like enzyme was measured as the consumption of NADPH (nmol \cdot min⁻¹ \cdot mg⁻¹ of protein) that reduces mercuric or uranyl ions. The values given are percentages of the highest activity monitored in the presence of DTT to fully reduce MerA, which was taken as 100%. The numbers are the mean values \pm standard deviations from four assays (two measurements performed on two independent enzyme extracts).

Consistently, MerA was shown to possess genuine NADPH-driven mercuric reductase activity, which requires residue C78 residue of its invariant redox motif (CX₄C) (Table 3). The high level of sequence homology between the MerA proteins from the bacterium *Geobacter uraniireducens* (GenBank accession number ZP_01142587) and *Synechocystis* suggested to us that the *Synechocystis* MerA enzyme might also operate in protection against uranyl ions. Indeed, MerA was found to possess a NADPH-driven uranyl reductase activity (Table 3) that is crucial to uranium tolerance (Fig. 2). This is the first report of an enzyme displaying both mercuric and uranyl reductase activities. Challenging the notion of metal selectivity, such cyanobacterial enzymes with the capacity to remediate at least mercury and uranium, two frequent pollutants (15–17), might be of value for future bioindication and/or bioremediation purposes, as most polluted sites contain cocktails of toxic metals.

Also, interestingly, Grx1 was found to be involved in the defense of *Synechocystis* against both Hg and U, in agreement with the Grx1-MerA interaction (Fig. 2). Furthermore, the C86 residue of Grx1, which is crucial to its interaction with MerA, was shown to be critical for cell protection against both Hg and U (Fig. 2). To our knowledge, this is the first report that a Grx enzyme operates in defense against both mercury and uranium. As a negative control, we verified that Grx2, which does not interact with MerA (Table 2), is involved in neither Hg nor U tolerance (Fig. 2). Grx2, but not Grx1, was found to interact with ArsC, the arsenate reductase enzyme (Table 2), which can be glutathionylated upon arsenate reduction and subsequently reactivated through deglutathionylation catalyzed by the heterologous *E. coli* GrxA enzyme (35). By analogy with these results, the presently reported MerA-Grx1 interaction led us to speculate that MerA might be glutathionylated upon Hg²⁺ reduction and subsequently deglutathionylated by Grx1. Indeed, MerA activity could be inhibited by glutathionylation (Table 3 and Fig. 3) and subsequently reactivated by Grx1 (Table 3). Furthermore, MerA activity appeared to be lower in the *grx1* null mutant than in the WT strain (Table 4). Moreover, the C31 (redox-active site) and C86 (MerA interaction) residues of Grx1 were found to be critical for MerA reactivation (Table 3). To our knowledge, this is the first report that mercuric reductase activity can be regulated by glutathionylation, under the control of a glutaredoxin likely catalyzing deglutathionylation. Collectively, our findings shed light on the selectivity of the Grx enzymes, an as yet poorly understood phenomenon in photosynthetic organisms (36). These findings are also important for emphasizing the evolutionary conservation of the glutathionylation/deglutathionylation process, so far described mostly for eukaryotes (19, 20, 37). In prokaryotes, only few proteins are known to be regulated via glutathionylation, namely MetE (methionine biosynthesis), phosphoadenylyl-sulfate (PAPS) reductase (sulfur assimilation), ArsC (arsenate reduction), and OxyR (transcriptional regulation) (38). We propose to include MerA in this list.

ACKNOWLEDGMENTS

We thank Daniel Ladant (Pasteur Institute, Paris, France) for the gift of the bacterial two-hybrid system, Pierre Genevoux for *E. coli* strain KY226, and Tania Arcondéguy for plasmid pMalC2.

This work was supported in part by the French scientific programs Toxicologie Nucléaire Environnementale, ANR Biosys06-134823: SULFIRHOM,

and ANR Blanc08-0153: GLUTAPHOTO. B.M., S.C., S.S., and M.B. were recipients of fellowships from the CEA (B.M.) and the ANR (S.C., S.S., and M.B.).

REFERENCES

- Narainsamy K, Marteyn B, Sakr S, Cassier-Chauvat C, Chauvat F. 2013. Genomics of the pleiotropic glutathione system in cyanobacteria, p. 157–188. In Cassier-Chauvat C, Chauvat F (ed), Genomics of cyanobacteria, vol 65. Elsevier Academic Press, New York, NY.
- Lillig CH, Berndt C. 21 December 2012. Glutaredoxins in thiol/disulfide exchange. *Antioxid. Redox Signal.* doi:10.1089/ars.2012.5007.
- Marteyn B, Domain F, Legrain P, Chauvat F, Cassier-Chauvat C. 2009. The thioredoxin reductase-glutaredoxins-ferredoxin crossroad pathway for selenate tolerance in *Synechocystis* PCC6803. *Mol. Microbiol.* 71:520–532.
- Johansson C, Lillig CH, Holmgren A. 2004. Human mitochondrial glutaredoxin reduces S-glutathionylated proteins with high affinity accepting electrons from either glutathione or thioredoxin reductase. *J. Biol. Chem.* 279:7537–7543.
- Zaffagnini M, Michelet L, Massot V, Trost P, Lemaire SD. 2008. Biochemical characterization of glutaredoxins from *Chlamydomonas reinhardtii* reveals the unique properties of a chloroplastic CGFS-type glutaredoxin. *J. Biol. Chem.* 283:8868–8876.
- Herrero E, Belli G, Casa C. 2010. Structural and functional diversity of glutaredoxins in yeast. *Curr. Protein Pept. Sci.* 11(8):659–668.
- Rouhier N, Couturier J, Johnson MK, Jacquot JP. 2010. Glutaredoxins: roles in iron homeostasis. *Trends Biochem. Sci.* 35:43–52.
- Lill R, Hoffmann B, Molik S, Pierik AJ, Rietzschel N, Stehling O, Uzarska MA, Webert H, Wilbrecht C, Muhlenhoff U. 2012. The role of mitochondria in cellular iron-sulfur protein biogenesis and iron metabolism. *Biochim. Biophys. Acta* 1823:1491–1508.
- Tamarit J, Belli G, Cabisco E, Herrero E, Ros J. 2003. Biochemical characterization of yeast mitochondrial Grx5 monothiol glutaredoxin. *J. Biol. Chem.* 278:25745–25751.
- Michelet L, Zaffagnini M, Massot V, Keryer E, Vanacker H, Miginiac-Maslow M, Issakidis-Bourguet E, Lemaire SD. 2006. Thioredoxins, glutaredoxins, and glutathionylation: new crosstalks to explore. *Photosynth. Res.* 89:225–245.
- Piccicocchi A, Saguez C, Boussac A, Cassier-Chauvat C, Chauvat F. 2007. CGFS-type monothiol glutaredoxins from the cyanobacterium *Synechocystis* PCC6803 and other evolutionary distant model organisms possess a glutathione-ligated [2Fe-2S] cluster. *Biochemistry* 46:15018–15026.
- Lopez-Maury L, Sanchez-Riego AM, Reyes JC, Florencio FJ. 2009. The glutathione/glutaredoxin system is essential for arsenate reduction in *Synechocystis* sp. strain PCC 6803. *J. Bacteriol.* 191:3534–3543.
- Lefebvre DD, Kelly D, Budd K. 2007. Biotransformation of Hg(II) by cyanobacteria. *Appl. Environ. Microbiol.* 73:243–249.
- Lorenz MG, Krumbein WE. 1985. Influence of leaching parameters on the biological removal of uranium from coal by a filamentous cyanobacterium. *Appl. Environ. Microbiol.* 50:1296–1300.
- Ariya PA, Dastoor AP, Amyot M, Schroeder WH, Barrie L, Anlauf K, Raofie F, Ryzhkov A, Davignon D, Lalonde J, Steffen A. 2004. The article: a sink for mercury. *Tellus B Chem. Phys. Meteorol.* 56:397–403.
- Clarkson TW, Magos L. 2006. The toxicology of mercury and its chemical compounds. *Crit. Rev. Toxicol.* 36:609–662.
- Wall JD, Krumholz LR. 2006. Uranium reduction. *Annu. Rev. Microbiol.* 60:149–166.
- De Philippis R, Colica G, Micheletti E. 2011. Exopolysaccharide-producing cyanobacteria in heavy metal removal from water: molecular basis and practical applicability of the biosorption process. *Appl. Microbiol. Biotechnol.* 92:697–708.
- Dalle-Donne I, Rossi R, Colombo G, Giustarini D, Milzani A. 2009. Protein S-glutathionylation: a regulatory device from bacteria to humans. *Trends Biochem. Sci.* 34:85–96.
- Zaffagnini M, Bedhomme M, Marchand CH, Morisse S, Trost P, Lemaire SD. 2012. Redox regulation in photosynthetic organisms: focus on glutathionylation. *Antioxid. Redox Signal.* 16(6):567–586.
- Rippka R, Deruelles J, Waterbury JB, Herdman M, Stanier RY. 1979. Generic assignments, strains histories and properties of pure cultures of cyanobacteria. *J. Gen. Microbiol.* 111:1–61.
- Domain F, Houot L, Chauvat F, Cassier-Chauvat C. 2004. Function and regulation of the cyanobacterial genes *lexA*, *recA* and *ruvB*: LexA is critical

- to the survival of cells facing inorganic carbon starvation. *Mol. Microbiol.* 53:65–80.
23. Kanemori M, Nishihara K, Yanagi H, Yura T. 1997. Synergistic roles of HslVU and other ATP-dependent proteases in controlling in vivo turnover of sigma32 and abnormal proteins in *Escherichia coli*. *J. Bacteriol.* 179:7219–7225.
 24. Karimova G, Pidoux J, Ullmann A, Ladant D. 1998. A bacterial two-hybrid system based on a reconstituted signal transduction pathway. *Proc. Natl. Acad. Sci. U. S. A.* 95:5752–5756.
 25. Labarre J, Chauvat F, Thuriaux P. 1989. Insertional mutagenesis by random cloning of antibiotic resistance genes into the genome of the cyanobacterium *Synechocystis* PCC6803. *J. Bacteriol.* 171:3449–3457.
 26. Fox B, Walsh CT. 1982. Mercuric reductase. Purification and characterization of a transposon-encoded flavoprotein containing an oxidation-reduction-active disulfide. *J. Biol. Chem.* 257:2498–2503.
 27. Lillig CH, Potamitou A, Schwenn JD, Vlami-Gardikas A, Holmgren A. 2003. Redox regulation of 3'-phosphoadenylylsulfate reductase from *Escherichia coli* by glutathione and glutaredoxins. *J. Biol. Chem.* 278:22325–22330.
 28. Bedhomme M, Zaffagnini M, Marchand CH, Gao XH, Moslonka-Lefebvre M, Michelet L, Decottignies P, Lemaire SD. 2009. Regulation by glutathionylation of isocitrate lyase from *Chlamydomonas reinhardtii*. *J. Biol. Chem.* 284:36282–36291.
 29. Marbouty M, Saguez C, Cassier-Chauvat C, Chauvat F. 2009. ZipN, a FtsA-like orchestrator of divisome assembly in the model cyanobacterium *Synechocystis* PCC6803. *Mol. Microbiol.* 74:409–420.
 30. Fernandes AP, Holmgren A. 2004. Glutaredoxins: glutathione-dependent redox enzymes with functions far beyond a simple thioredoxin backup system. *Antioxid. Redox Signal.* 6(1):63–74.
 31. Silver S, Phung L. 2005. A bacterial view of the periodic table: genes and proteins for toxic inorganic ions. *J. Ind. Microbiol. Biotechnol.* 32:587–605.
 32. Mermet-Bouvier P, Chauvat F. 1994. A conditional expression vector for the cyanobacteria *Synechocystis* sp. PCC6803 and PCC6714 or *Synechococcus* sp. PCC7942 and PCC6301. *Curr. Microbiol.* 28:145–148.
 33. Poncelet M, Cassier-Chauvat C, Leschelle X, Bottin H, Chauvat F. 1998. Targeted deletion and mutational analysis of the essential (2Fe-2S) plant-like ferredoxin in *Synechocystis* PCC6803 by plasmid shuffling. *Mol. Microbiol.* 28:813–821.
 34. Marraccini P, Bulteau S, Cassier-Chauvat C, Mermet-Bouvier P, Chauvat F. 1993. A conjugative plasmid vector for promoter analysis in several cyanobacteria of the genera *Synechococcus* and *Synechocystis*. *Plant Mol. Biol.* 23:905–909.
 35. Li R, Haile JD, Kennelly PJ. 2003. An arsenate reductase from *Synechocystis* sp. strain PCC 6803 exhibits a novel combination of catalytic characteristics. *J. Bacteriol.* 185:6780–6789.
 36. Couturier J, Jacquot JP, Rouhier N. 2009. Evolution and diversity of glutaredoxins in photosynthetic organisms. *Cell. Mol. Life Sci.* 66:2539–2557.
 37. Gallogly MM, Mieyal JJ. 2007. Mechanisms of reversible protein glutathionylation in redox signaling and oxidative stress. *Curr. Opin. Pharmacol.* 7:381–391.
 38. Masip L, Veeravalli K, Georgiou G. 2006. The many faces of glutathione in bacteria. *Antioxid. Redox Signal.* 8(5–6):753–762.
 39. Prentki P, Binda A, Epstein A. 1991. Plasmid vectors for selecting IS1-promoted deletions in cloned DNA: sequence analysis of the omega interposon. *Gene* 103:17–23.